

## Vesicles generated during storage of red cells are rich in the lipid raft marker stomatin

Ulrich Salzer, Rong Zhu, Marleen Luten, Hirotaka Isobe, Vassili Pastushenko, Thomas Perkmann, Peter Hinterdorfer, and Giel J.C.G.M. Bosman

**BACKGROUND:** The release of vesicles by red blood cells (RBCs) occurs in vivo and in vitro under various conditions. Vesiculation also takes place during RBC storage and results in the accumulation of vesicles in RBC units. The membrane protein composition of the storage-associated vesicles has not been studied in detail. The characterization of the vesicular membrane might hint at the underlying mechanism of the storage-associated changes in general and the vesiculation process in particular.

**STUDY DESIGN AND METHODS:** Vesicles from RBCs that had been stored for various periods were isolated and RBCs of the same RBC units were used to generate calcium-induced microvesicles. These two vesicle types were compared with respect to their size with atomic force microscopy, their raft protein content with detergent-resistant membrane (DRM) analysis, and their thrombogenic potential and activity with annexin V binding and thrombin generation, respectively.

**RESULTS:** The storage-associated vesicles and the calcium-induced microvesicles are similar in size, in thrombogenic activity, and in membrane protein composition. The major differences were the relative concentrations of the major integral DRM proteins. In storage-associated vesicles, stomatin is twofold enriched and flotillin-2 is threefold depleted.

**CONCLUSION:** These data indicate that a stomatin-specific, raft-based process is involved in storage-associated vesiculation. A model of the vesiculation process in RBCs is proposed considering the raft-stabilizing properties of stomatin, the low storage temperature favoring raft aggregation, and the previously reported storage-associated changes in the cytoskeletal organization.

Storage of RBCs causes various cellular changes that are assumed to contribute to the reduced viability of posttransfusion RBCs, the so-called "storage lesion." Stored RBCs show an increased osmotic fragility and a reduced deformability<sup>1,2</sup> and storage is accompanied by oxidative damage to cytoskeletal proteins and membrane lipids and by increased methemoglobin formation.<sup>3-5</sup> Moreover, vesiculation takes place during RBC storage under blood bank conditions.<sup>6</sup> In vivo, vesiculation takes place in a spleen-facilitated manner, thereby accounting for the loss of approximately 20 percent of the cell surface and an increase in cell density during the RBC life span.<sup>7,8</sup> Vesiculation is thought to be of functional importance as a defense mechanism of the RBC against complement-mediated lysis.<sup>9</sup> The amount of hemoglobin (Hb) in

**ABBREVIATIONS:** AChE = acetylcholinesterase;

DRM = detergent-resistant membrane; FWHM = full width at half-maximum; GPI = glycosylphosphatidylinositol; TBS = Tris-buffered saline; V<sub>ca</sub> = calcium-induced vesicles; V<sub>sto</sub> = storage-induced vesicles.

From the Max F. Perutz Laboratories and the Department of Vascular Biology and Thrombosis Research, Center for Biomolecular Medicine and Pharmacology, Medical University of Vienna, Vienna, Austria; the Institute of Biophysics, Johannes Kepler University, Linz, Austria; the Department of Research and Education, Sanquin Blood Bank Southeast Region, Nijmegen, the Netherlands; and the Department of Biochemistry, Nijmegen Center for Molecular Life Sciences, Radboud University Nijmegen Medical Center, the Netherlands.

Address reprint requests to: Ulrich Salzer, Max F. Perutz Laboratories, Medical University of Vienna, Dr Bohr-Gasse 9, A-1030 Vienna, Austria; e-mail: ulrich.salzer@meduniwien.ac.at.

This work was supported by the Austrian Science Fund (FWF, Grant P15486). We are grateful to Rainer Prohaska for helpful discussions and for critically reading the manuscript.

Received for publication July 3, 2007; revision received August 14, 2007, and accepted August 17, 2007.

doi: 10.1111/j.1537-2995.2007.01549.x.

TRANSFUSION 2008;48:451-462.

storage-associated vesicles exceeds the amount of extracellular free Hb caused by storage-associated cell lysis.<sup>10</sup> The progressive storage-induced loss of RBC surface area via vesicle release correlates with a decrease in the proper complex formation in vitro between the cytoskeletal components spectrin, actin, and protein 4.1.<sup>4</sup> Spectrin oxidation was suggested to be the underlying cause of this impairment as it closely correlates with vesicle accumulation in the storage medium.<sup>3</sup>

The storage-induced vesicles are depleted of the cytoskeletal proteins spectrin and ankyrin but contain the major transmembrane proteins band 3 and the glycoporphins.<sup>11</sup> Moreover, nearly all of the tested blood group antigens were found to be present on these vesicles.<sup>12,13</sup> A detailed analysis, however, comparing the relative amounts of membrane proteins and the antigen markers in the vesicular and the RBC membrane has not been performed. The segregation of RBC membrane proteins during calcium-induced vesiculation has been studied in more detail. Several factors such as 1) binding to the cytoskeleton,<sup>14,15</sup> 2) association with lipid rafts,<sup>16,17</sup> and 3) the intrinsic curvature of a molecule or of a molecular ensemble<sup>18</sup> are assumed to influence the segregation process of integral membrane proteins resulting in the observed enrichment and/or depletion of membrane proteins and lipids in the released vesicles. Various raft proteins are enriched in calcium-induced vesicles, and they were shown to be present in the detergent-resistant membrane (DRM) fraction of these vesicles.<sup>17</sup> These proteins are stomatin, an integral membrane protein that is monotonically associated with the cytoplasmic membrane leaflet;<sup>19,20</sup> acetylcholinesterase (AChE), an extracellular enzyme linked to the membrane via a glycosylphosphatidylinositol (GPI) anchor;<sup>16</sup> and synexin (annexin VII) and sorcin, two cytosolic proteins that associate with lipid rafts in a calcium-dependent manner.<sup>17</sup> Interestingly, flotillin-1 and flotillin-2, which are—after stomatin—the most abundant integral RBC raft proteins, are depleted from these calcium-induced vesicles. This finding indicates that different types of rafts coexist in the RBC membrane and that they segregate in the calcium-induced vesiculation process by as yet undetermined mechanisms.

To obtain insight into the processes that take place during storage-associated vesiculation, we isolated vesicles ( $V_{sto}$ ) from stored RBCs and calcium-induced vesicles ( $V_{ca}$ ) generated from RBCs of the same RBC unit and compared them with respect to their size, their protein, and their DRM composition. There is a general similarity between these vesicles and both vesicle types display procoagulant activity. The major difference is the larger enrichment of stomatin and the stronger depletion of the flotillins in  $V_{sto}$  compared to  $V_{ca}$ . Integrating these findings and previous data on storage-associated changes of the cytoskeleton, we propose a raft-based model for the vesiculation process during RBC storage.

## MATERIALS AND METHODS

### Reagents

Acetylthiocholine chloride, aprotinin, bestatin hydrochloride, 5,5'-dithiobis-(2-nitrobenzoic acid), leupeptin, pepstatin A, phenylmethylsulfonyl fluoride, *N*- $\alpha$ -tosyl-L-lysine chloromethyl ketone, *N*-tosyl-L-phenylalanine chloromethyl ketone, and Triton X-100 were from Sigma Chemical Co. (St Louis, MO). Analytical-grade laboratory chemicals were from Merck (Darmstadt, Germany), and reinforced nitrocellulose was Optitran BA-S 83 (Schleicher & Schuell, Dassel, Germany).

### Preparation of RBCs

RBCs were prepared as described previously.<sup>21</sup> Briefly, 500 mL of whole blood was collected in a quadruple CPD/SAGM top-and-bottom bag system (Composelect, Fresenius HemoCare, Emmer-Compascuum, the Netherlands) and anticoagulated with 70 mL of CPD. After cooling for at least 4 hours and centrifugation of the whole-blood unit, the blood was separated into its components (plasma, buffy coat, and RBCs) with an automated blood processing device (Compomat G4, Fresenius HemoCare). A total of 110 mL SAGM was transferred from the RBC storage bag to the RBCs before leukodepletion by in-line filtration. After filtration, RBCs were stored for 7 weeks at 2 to 6°C. From the first week of storage and weekly thereafter, a sample was collected from the stored units by a sterile sampling device, after gentle mixing of the unit content by inversion for approximately 5 minutes.

### Hematologic and biochemical measurements

RBC counts and total Hb concentration were measured with a hematology analyzer (Coulter Onyx, Beckman Coulter, Fullerton, CA; or Sysmex XT1800i, Sysmex Corporation, Kobe, Japan). Extracellular Hb concentration was determined by a colorimetric assay on a clinical chemistry system (Aeroset, Abbott Diagnostics, Abbott Park, IL). The percentage of hemolysis was calculated with the following formula

$$\text{Hemolysis} = 100 \text{ percent} \times ((1 - \text{Hct}) \times \text{extracellular Hb}) / \text{total Hb}.^{22,23}$$

Extracellular sodium and glucose were measured on a blood gas analyzer (Chiron 860/865, Bayer Diagnostics, Tarrytown, NJ). Potassium levels were measured in the extracellular fluid after centrifugation with the Abbott Aeroset. Adenine nucleotides were quantitatively assayed by anion-exchange high-performance liquid chromatography, as described by de Korte and colleagues.<sup>24,25</sup> The adenylate energy charge was calculated according to the formula  $((\text{ATP} + 1/2\text{ADP}) / (\text{ATP} + \text{ADP} + \text{AMP}))$ .

## Preparation of vesicles

### *Vesicles during storage ( $V_{sto}$ )*

Approximately 50 mL of RBCs (Hct approx. 60%) was mixed with 20 mL of Tris-buffered saline (TBS; 150 mmol/L NaCl, 10 mmol/L Tris-HCl, pH 7.4), and RBCs were pelleted (P1) by centrifugation at  $1850 \times g$  for 10 minutes. The supernatant (SN1) was centrifuged at  $28,000 \times g$  for 35 minutes; the supernatant (SN2) was removed and the pelleted material (P2) was resuspended in 1 mL of TBS for further subfractionation. A first centrifugation step ( $15,000 \times g$ , 25 sec) removed contaminating RBCs and large vesicles (P3) and the resulting supernatant (SN3) was subjected to two further centrifugation steps. Upon centrifugation at  $15,000 \times g$  for 7 minutes a red vesicle pellet (P4) was obtained, which was overlaid with a white layer of contaminating ghosts. The supernatant (SN4) was kept for further processing, and the ghosts were carefully removed from the top of P4. The vesicle pellet P4 was then resuspended in 1 mL of TBS, mixed with SN4, and recentrifuged at  $100,000 \times g$  for 20 minutes. The final vesicle pellet (P5) corresponding to  $V_{sto}$  was resuspended in an appropriate volume of TBS.

### *Vesicles after calcium/ionophore treatment ( $V_{ca}$ )*

Vesicles were prepared as described<sup>17</sup> with minor modifications. Briefly, RBCs of the respective RBC units were washed in TBS; resuspended in 9 volumes of TBS, 1 mmol per L  $\text{CaCl}_2$ , and 5  $\mu\text{mol}$  per L ionophore A23187; and incubated at 37°C for 30 minutes under constant agitation. RBCs were pelleted at  $16,000 \times g$  for 20 seconds. The supernatant was then centrifuged for 30 minutes at  $16,000 \times g$ . The vesicle pellet was resuspended in 1 mL of TBS, and the two centrifugation steps were repeated to remove contaminating RBCs. The final vesicle pellet corresponding to  $V_{ca}$  was resuspended in an appropriate volume of TBS.

## Protein analyses

Protein samples were analyzed by gel electrophoresis, silver staining, immunoblotting with the indicated antibodies, and determination of AChE activity, respectively, as previously described.<sup>17</sup> Quantitative immunoblotting was performed by directly comparing aliquots of vesicle samples normalized to total vesicular protein content and several dilutions thereof. Protein amounts were determined by a photometric protein assay (Bio-Rad, Hercules, CA).

## Flotation assay

The flotation assay of the vesicles was performed as previously described with some modifications.<sup>17</sup> Briefly, 80  $\mu\text{L}$

of vesicle suspension was lysed by addition of 20  $\mu\text{L}$  of 2.5 percent Triton X-100 and proteinase inhibitors (20  $\mu\text{g}/\text{mL}$  bestatin hydrochloride, 25  $\mu\text{g}/\text{mL}$  *N*- $\alpha$ -tosyl-L-lysine chloromethyl ketone, 40  $\mu\text{g}/\text{mL}$  *N*-tosyl-L-phenylalanine chloromethyl ketone, 20  $\mu\text{g}/\text{mL}$  phenylmethylsulfonyl fluoride,  $\mu\text{g}/\text{mL}$  pepstatin A, 40  $\mu\text{g}/\text{mL}$  leupeptin hemisulfate, 10  $\mu\text{g}/\text{mL}$  aprotinin) in TBS, incubated for 20 minutes on ice, and mixed with 100  $\mu\text{L}$  of 80 percent sucrose in TBS. The resulting suspension was placed in centrifuge tubes (13  $\times$  51 mm, Beckman), overlaid with 1900  $\mu\text{L}$  of 35 percent sucrose in TBS and 350  $\mu\text{L}$  of 5 percent sucrose in TBS, and centrifuged in a precooled rotor (SW50.1, Beckman) at  $230,000 \times g$  and 4°C for 17 hours. Six fractions were collected from the top. Aliquots were analyzed by immunoblotting and by measuring their AChE activity.

## Atomic force microscopy

A magnetically driven dynamic-force microscope (Macmode PicoSPM, Molecular Imaging, Phoenix, AZ) was used. The topography images were recorded in the Magnetic AC (Mac) mode<sup>26,27</sup> with cantilevers (MacLevers, Molecular Imaging, Tempe, AZ) of approximately 0.03 N per m nominal spring constant in aqueous buffer solutions at room temperature. Measurements were performed with approximately 10-nm free-tip oscillation amplitude at approximately 3-kHz driving frequency, and the feedback loop was driven at approximately 26 percent amplitude reduction. Image size was 4  $\times$  4  $\mu\text{m}$  at 0.5-Hz lateral scan rate. Vesicles were specifically bound to wheat germ agglutinin (WGA)-coated mica surfaces. For this, mica sheets (Gröpl, Tulln, Austria) were first derivatized with ethanolamine as previously described<sup>28,29</sup> and then incubated for 1.5 hours with a solution of 1 mg per mL ethylene glycol-bis(succinimidylsuccinate) (Pierce, Rockford, IL) in chloroform containing 0.5 percent triethylamine, washed in chloroform, and dried with nitrogen. Subsequently, a solution of 0.5 mg per mL WGA (Sigma) in 10 mmol per L sodium phosphate and 150 mmol per L NaCl, pH 7.5 (phosphate-buffered saline [PBS]), was applied for 2 hours, and the excess of WGA was removed. Finally, the vesicles were bound to the mica surface in HEPES-buffered saline (5 mmol/L HEPES, 150 mmol/L NaCl, pH 7.3) for 15 minutes at appropriate concentrations and imaged in the same buffer by means of atomic force microscopy. The diameter of the vesicles was calculated from the full width at half-maximum (FWHM) as illustrated in Fig. 3 with the angle  $\theta$  of cantilever tip as 18°. The tip radius was estimated through measuring the atomic force microscopy image of HRV2 virus, which has a known diameter of approximately 30 nm. From the measurement, it was found that the vesicle was pressed in the scanning direction before the cantilever tip reached the highest point of the vesicle. Therefore, only the second

half of the FWHM was used to calculate the diameter of the vesicle.

### Thrombin generation assay

Ten microliters of the vesicle suspension ( $1 \times 10^4$  microvesicles) was mixed with 40  $\mu\text{L}$  of 1 mmol per L fluorogenic thrombin substrate Z-Gly-Gly-Arg-AMC (Bachem AG, Bubendorf, Switzerland), 10  $\mu\text{L}$  of 75 mmol per L  $\text{CaCl}_2$ , and 10  $\mu\text{L}$  of HEPES buffer (5 mg/mL bovine serum albumin, 25 mmol/L HEPES, pH 7.35, 175 mmol/L NaCl). The *in vitro* thrombin generation was started by adding 30  $\mu\text{L}$  37°C prewarmed of human vesicle-free plasma obtained from whole blood containing 18.3  $\mu\text{g}$  per mL corn trypsin inhibitor (Haematological Technologies, Inc., Essex Junction, VT) to prevent artificial contact dependent preactivation of Factor XII.<sup>30</sup> The increase of the fluorescence intensity, which is proportional to the concentration of the generated thrombin, was measured continuously every minute up to 60 minutes with a microplate fluorescence reader (Wallac 1420 multilabel counter, Wallac/Perkin-Elmer, Turku, Finland) with an excitation wavelength of 355 nm and an emission wavelength of 460 nm. The increase of fluorescence intensity per minute was calculated and converted to thrombin concentrations (nmol/L) with a reference curve obtained by measuring the rate of substrate conversion by purified human  $\alpha$ -thrombin.<sup>31</sup>

### Flow cytometry

For analysis of annexin V binding to vesicles, microvesicles were stained with phycoerythrin (PE)-conjugated annexin V (BD Biosciences Pharmingen, San Jose, CA) diluted 1:40 in binding buffer (40 mmol/L NaCl, 10 mmol/L HEPES/NaOH, pH 7.4) either in the presence (2.5 mmol/L  $\text{CaCl}_2$ ) or in the absence of calcium. Incubation was carried out for 30 minutes in the dark at room temperature. After being washed, labeled vesicles were resuspended in PBS and analyzed by flow cytometry on a cell sorter (FACSort, BD, Franklin Lakes, NJ). At least 3000 events per sample were acquired and analyzed with computer software (CellQuest, BD).

## RESULTS

Homeostasis of RBCs becomes increasingly impaired upon RBC storage. An exponential increase in the hemolysis rate is observed at prolonged storage times. There are marked changes in the extracellular cation concentrations with an increase in the proton and potassium and a decrease in the sodium ion concentration. These variables are associated with a gradual increase of the MCV indicating a progressive impairment of cell volume regulation. The storage-associated progressive loss of energy is high-

lighted by the decrease in the intracellular ATP level and the adenylate energy charge of the cells, which probably accounts for most of the observed changes (Fig. 1).

Storage-induced microvesicles ( $V_{\text{sto}}$ ) were isolated from RBCs that had been stored for 4, 14, and 50 days and RBCs from these RBC units were used to prepare calcium-induced microvesicles ( $V_{\text{ca}}$ ). Our  $V_{\text{sto}}$  preparation protocol was designed to avoid the presence of contaminating RBCs and ghosts and therefore includes further purification steps of the vesicles isolated by the first high-speed centrifugation step (see Materials and Methods). Compared to RBCs stored for 4 days, there is a 2- and 15-fold increase in the amount of  $V_{\text{sto}}$  when RBCs are stored for 14 and 50 days, respectively (Fig. 2), showing a strong increase of vesicle generation at prolonged storage times.

We used atomic force microscopy to compare the heights and diameters of  $V_{\text{sto}}$  and  $V_{\text{ca}}$ . The radii of the cantilever tip were determined by use of the well-defined size of the human rhinovirus as a calibrating measure,<sup>32</sup> and the diameters of the vesicles were calculated from the FWHM data as indicated in Fig. 3 with the angle  $\theta$  of the cantilever tip as 18°. This provides a good correlation between the distributions of the heights and the diameters within the vesicle population. The topography images of the atomic force experiments (Fig. 3) show that the sizes of  $V_{\text{sto}}$  and  $V_{\text{ca}}$  isolated from the same RBCs are comparable. The number of vesicles with heights and diameters of greater than 140 nm, however, is larger in the  $V_{\text{sto}}$  than in  $V_{\text{ca}}$  population. Moreover, the peaks of the distribution of the diameters slightly differ, with  $V_{\text{sto}}$  being about 10 nm larger than  $V_{\text{ca}}$ . We observed a small variation in the size distributions of  $V_{\text{sto}}$  of different storage time spans (data not shown), which is probably due to donor-related variations. Because in this study purity of the  $V_{\text{sto}}$  pool was more important than its completeness, we omitted the P3 pellet (see Materials and Methods) containing—apart from contaminating RBCs—also a population of larger vesicles. This explains the low amount of  $V_{\text{sto}}$  larger than 200 nm, compared to the vesicle preparation of Greenwalt and coworkers.<sup>11</sup> Moreover, the tip size correction in this work accounts for the difference to our previous data on the size distribution of microvesicles ( $V_{\text{ca}}$ ) with uncorrected FWHM data.<sup>17</sup>

To learn about the segregation of membrane proteins in the storage-induced vesiculation process, we compared the protein patterns of these vesicles to  $V_{\text{ca}}$  and RBC membranes of the same RBC units by sodium dodecyl sulfate (SDS)-polyacrylamide gel electrophoresis (PAGE) and silver staining (Fig. 4). Immunoblotting analyses of these samples indicated a differential behavior of the major raft marker proteins stomatin, flotillin-1, and flotillin-2 in the vesiculation processes. Whereas stomatin is enriched in both types of vesicles when compared to its relative abundance at the RBC membrane, flotillin-1 and flotillin-2 are depleted from the vesicles (data not shown). These

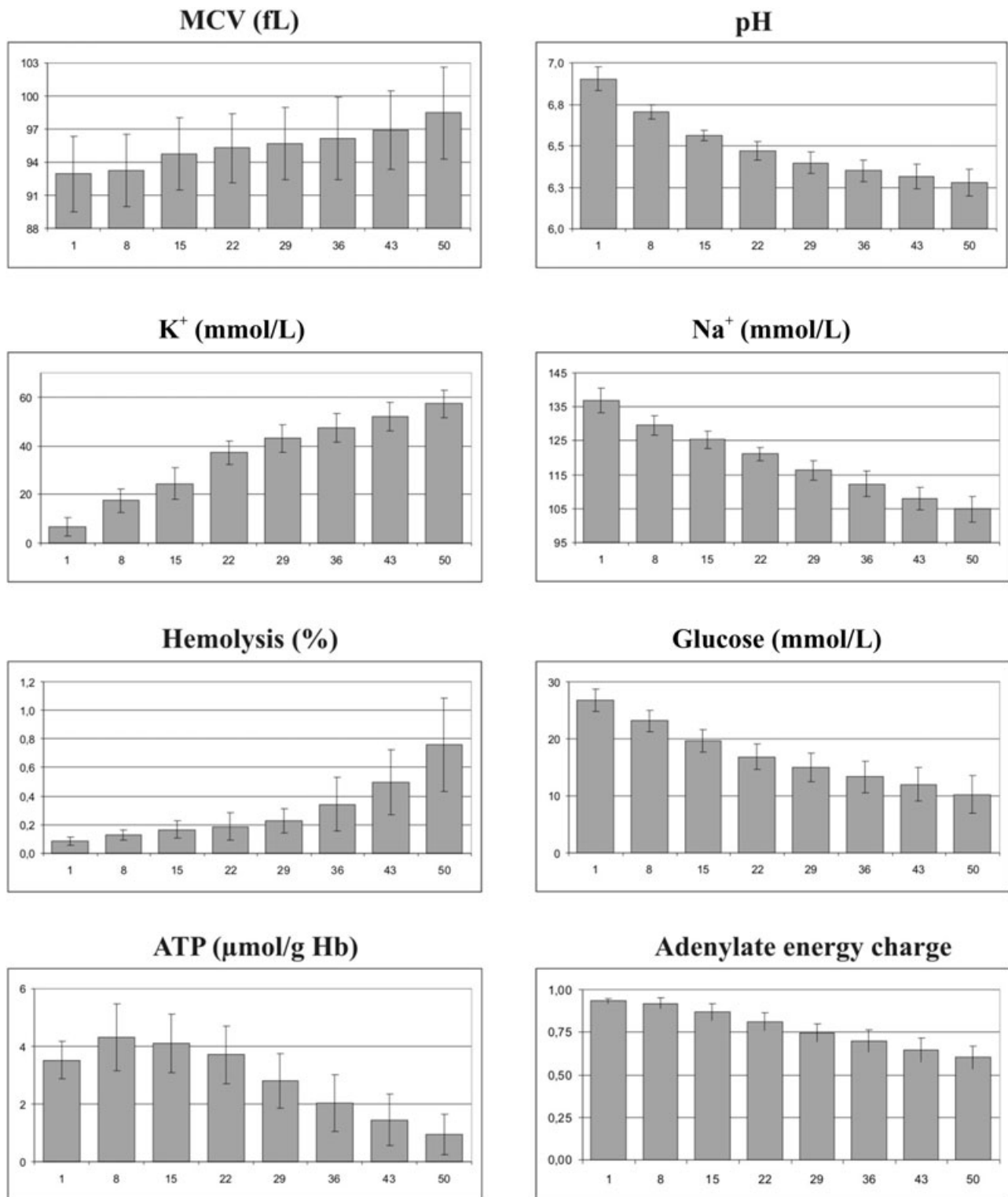


**Fig. 1.** Storage-associated changes in RBCs. RBCs were prepared from blood of healthy donors and stored at 2 to 6°C. Aliquots were collected at the indicated time points and the respective hematologic and biochemical measurements were performed as described under Materials and Methods. The numbers on the x axis of the graphs denote the storage time in days. Mean values and standard deviations (SDs) are shown ( $n = 11$  and  $n = 3$  for the ATP and the adenylate energy charge determinations, respectively).

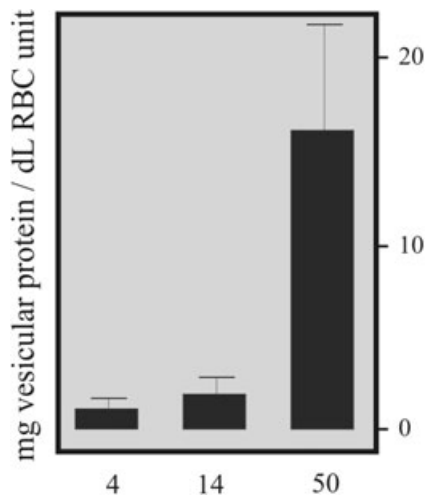


**Fig. 2.** Protein amount of vesicles generated during RBC storage.  $V_{sto}$  were isolated from RBC units stored for the indicated time spans and the amount of total vesicular protein was determined. The numbers on the x axis denote the storage time in days. The data depict the mean values and respective SDs of five independent experiments.

**TABLE 1.** Comparison of the amounts of selected membrane proteins between  $V_{sto}$  and  $V_{ca}$ \*

$V_{sto}/V_{ca}$	4 days	14 days	50 days
Band 3	0.9 ± 0.1	0.9 ± 0.2	0.9 ± 0.3
CD55	0.4 ± 0.1	0.5 ± 0.1	0.8 ± 0.3
AChE	0.6 ± 0.1	0.6 ± 0.1	0.8 ± 0.2
Flotillin-2	0.3 ± 0.1	0.3 ± 0.1	0.5 ± 0.1
Stomatin	1.9 ± 0.2	2.0 ± 0.1	2.1 ± 0.6

\* The ratios of the amounts of respective membrane proteins in  $V_{sto}$  and  $V_{ca}$  isolated at indicated times were determined by quantitative immunoblotting. Values greater than 1 indicate a relative enrichment of the protein in  $V_{sto}$  compared to  $V_{ca}$  and vice versa. The data are the mean values and respective SDs of four independent experiments.

analyses also indicated that the relative enrichment and/or depletion of these proteins differ between the  $V_{sto}$  and  $V_{ca}$ . To analyze the relative amounts of selected membrane proteins in  $V_{sto}$  and  $V_{ca}$  with more accuracy, we performed a semiquantitative immunoblotting analysis. The results confirm that stomatin is enriched about twofold in  $V_{sto}$  compared to  $V_{ca}$  (Table 1). In contrast, all the other proteins analyzed are diminished in  $V_{sto}$  than in  $V_{ca}$ , with the amount of flotillin-2 being about three times reduced compared to  $V_{ca}$ . The differences in the specific protein amounts between these vesicles decrease with prolonged storage times. Lipid-raft association is a common feature of these proteins, whereas only a small fraction of band 3 is supposed to be in rafts,<sup>15,33</sup> stomatin, flotillin-2, and the GPI-linked proteins AChE and CD55 are major integral raft components in RBCs.<sup>20</sup> It was previously shown that a segregation of stomatin and flotillin-2 takes place during

calcium-induced microvesiculation of RBCs.<sup>15,17</sup> The present data (Table 1) reveal that the segregation of these proteins is much more pronounced during the storage-associated vesiculation.

The presence of high amounts of stomatin in  $V_{sto}$  indicates that lipid rafts might be involved in  $V_{sto}$  vesiculation. Therefore, we sought vesicular membrane components that resist solubilization by Triton X-100 and float to low densities upon density gradient ultracentrifugation (DRMs). DRMs could be isolated from  $V_{sto}$  of all storage periods (Fig. 5). The distribution patterns of the various raft markers within the gradients are very similar in  $V_{sto}$  and  $V_{ca}$  isolated from the same RBC units. The major amount of stomatin and virtually all of flotillin-2 is DRM-associated (Density Fractions 1-3 in Fig. 5A, Fraction 1 in Fig. 5B) whereas only minor amounts of these proteins are found to be soluble (Density Fractions 4-6 in Fig. 5A, Fraction s in Fig. 5B). More than two-thirds of the AChE activity and about half of CD55 is associated with DRMs. Band 3 is absent from the low-density region of the gradients, supporting previous data that the major part of this protein is not raft-associated. In  $V_{sto}$  isolated from RBCs that had been stored for 50 days, however, a considerable fraction of band 3 is DRM-associated (Fig. 5A). The Duffy antigen that was previously shown to be present in DRMs from RBCs and vacuolar malaria parasites<sup>34</sup> is absent from DRMs derived from vesicles.

Because RBC-derived vesicles may have an effect on coagulation,<sup>35-37</sup> we measured the thrombogenic activity of different RBC vesicles in vitro. Both  $V_{ca}$  and  $V_{sto}$  were potent inducers of thrombin generation (Figs. 6A and 6B), whereas vesicles obtained by ATP depletion were not (data not shown). The pattern of thrombin generation as indicated by the lag phase and peak height induced by  $V_{sto}$  was similar to that of  $V_{ca}$ . The initiation and amplification of coagulation processes are strictly dependent on the availability of anionic phospholipids; therefore, we examined the extent of phosphatidylserine surface exposure on vesicles by means of annexin V binding (Figs. 6C and 6D). Approximately one-third of both  $V_{ca}$  and  $V_{sto}$  were positive for annexin V without showing a relevant difference in the mean fluorescence intensity between  $V_{ca}$  and  $V_{sto}$ , indicating a similar surface exposure of phosphatidylserine on  $V_{sto}$  and  $V_{ca}$ .

## DISCUSSION

It has long been noticed that Hb-containing vesicles are generated during blood storage.<sup>6,13,38</sup> The amount of vesiculation is influenced by the storage conditions and is reduced by leukoreduction.<sup>39-41</sup> We used a standard procedure for RBC preparation and storage following Dutch blood bank protocols.<sup>21</sup> To evaluate whether there are time-dependent changes in the generation and protein

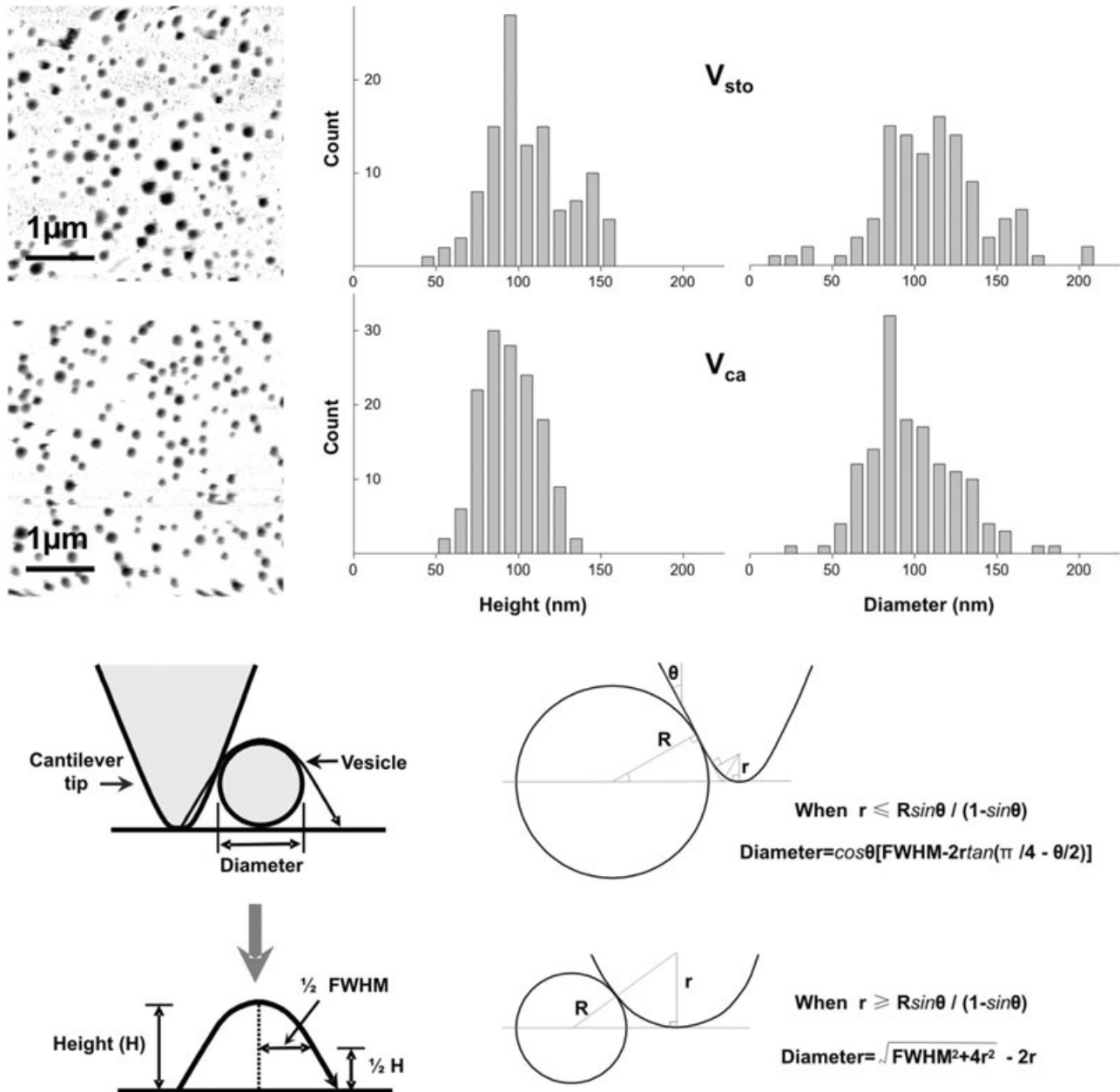
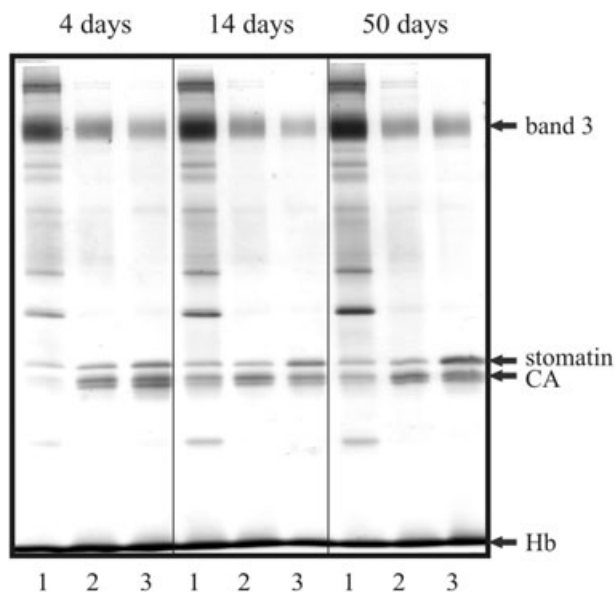


Fig. 3.  $V_{sto}$  and  $V_{ca}$  show a similar size distribution. Typical results of atomic force microscopy (AFM) measurements of  $V_{sto}$  and  $V_{ca}$  prepared from RBCs that had been stored for 50 days are presented. The first column shows the topography images of the vesicles, whereas the second and the third columns show the statistic distribution of the measured height and the calculated diameter of the vesicles, respectively. The diameter of the vesicle is calculated from the FWHM, as illustrated in the lower part.

composition of the vesicles, we focused on vesicles generated during RBC storage for 4, 14, and 50 days. Vesicles are already present in RBCs stored for 4 days indicating a continuous storage-dependent vesiculation process (Fig. 2). Because the ATP levels have not decreased after 4 days (Fig. 1), this observation is in accordance with data showing that vesiculation during short-term blood storage is independent of the cellular ATP level.<sup>3</sup> After 14 to 21 days of storage, however, there is an exponential

release of vesicles that might be due to energy depletion. In accordance with previous reports,<sup>41,42</sup> we find a significant negative correlation between the ATP content and the vesicle amount in the RBCs ( $r = -0.93$ ;  $p < 0.001$ ;  $n = 5$ ). A model by Gov and Safran<sup>43</sup> and Sens and Gov<sup>44</sup> proposes that diminishing ATP levels are associated with increasing compressive forces imposed by the cytoskeleton on the RBC membrane, which might be the cause for increased vesiculation.



**Fig. 4.** Protein amount and composition of vesicles generated during RBC storage.  $V_{sto}$  were isolated from RBC units stored for the indicated time spans and RBCs of the respective RBC units were used to generate RBC membranes and  $V_{ca}$ . RBC membranes (1),  $V_{ca}$  (2), and  $V_{sto}$  (3) were analyzed by 11 percent PAGE and silver staining. The ghost aliquots contained membranes of  $1.0 \times 10^7$  cells, and the vesicle aliquots were normalized to 12  $\mu$ g of total vesicular protein. Arrows indicate the positions of the respective protein bands (CA = carbonic anhydrase).

Recently, it was shown that lysophosphatidic acid induces vesicle release in RBCs and it was suggested that these vesicles are of (patho-)physiologic importance due to their thrombogenic activity.<sup>37</sup> Here we show that  $V_{sto}$  also display procoagulant activity with a thrombogenic activity that is similar to that of  $V_{ca}$  (Fig. 6). Annexin V binding assays reveal that both vesicle types expose similar amounts of phosphatidylserine. Both calcium-dependent and calcium-independent mechanisms of phosphatidylserine exposure in RBCs have been described.<sup>37,45</sup> Prolonged RBC storage does only slightly increase phosphatidylserine exposure in RBCs.<sup>46</sup> It is conceivable that the thrombogenic activity of  $V_{sto}$  arises from the loss of ATP-dependent aminophospholipid translocase activity due to metabolic depletion of the vesicles. The exponential increase of these procoagulant vesicles at prolonged storage times suggests that it should be considered to include the number of vesicles in the safety guidelines for stored RBC units.

The membrane of  $V_{ca}$  has previously been shown to be enriched in stomatin and AChE and to be depleted of band 3, flotillin-2, and aquaporin-1 compared to the RBC membrane.<sup>14,15,17,47</sup> Here, we show that there is a similar depletion of band 3 in  $V_{sto}$  and in  $V_{ca}$ , whereas the GPI-

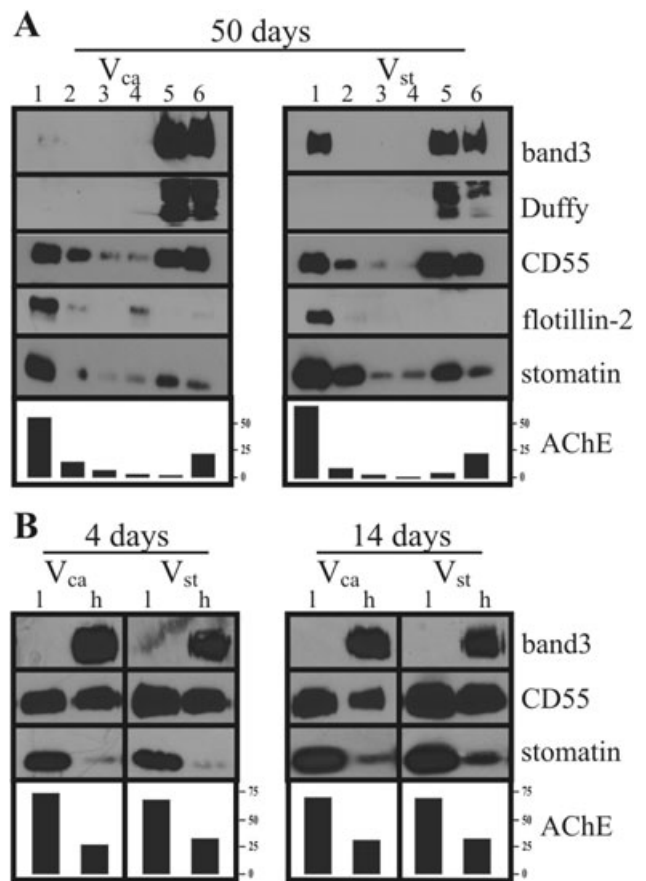


**Fig. 5.** DRMs of  $V_{sto}$  and  $V_{ca}$ .  $V_{sto}$  and  $V_{ca}$  were prepared from RBC units that had been stored for the indicated periods, lysed in 0.5 percent Triton X-100, and subjected to density gradient ultracentrifugation as described under Materials and Methods. Six fractions were collected from the top. (A) Aliquots of equal volumes were analyzed by SDS-PAGE and immunoblotting as indicated or for AChE activity; (B) Fractions 1 to 3 comprising the low-density region (l) and 4 to 6 comprising the high-density region (h) of the gradient were pooled and analyzed as in (A). Representative data of a set of three experiments are shown.

linked proteins AChE and CD55 are less enriched in  $V_{sto}$  than in  $V_{ca}$  (Table 1). The vesicle amounts used for the comparative analyses (Fig. 4 and Table 1) are normalized to a volume-dependent parameter (total vesicular protein). Because the vesicle diameters of the  $V_{ca}$  and  $V_{sto}$  are quite similar (Fig. 3) these data also reflect approximately equal vesicular surface areas. The relative enrichment of AChE in  $V_{ca}$  relative to phospholipids has been determined to be approximately 3-fold;<sup>14,47,48</sup> hence, the relative AChE/phospholipid enrichment in  $V_{sto}$  compared to RBC membranes can be roughly determined to be 2-fold. Interestingly, the enrichment of stomatin is higher and the depletion of flotillin-2 is even more pronounced in  $V_{sto}$  than in  $V_{ca}$ . Combining the data from Table 1 with

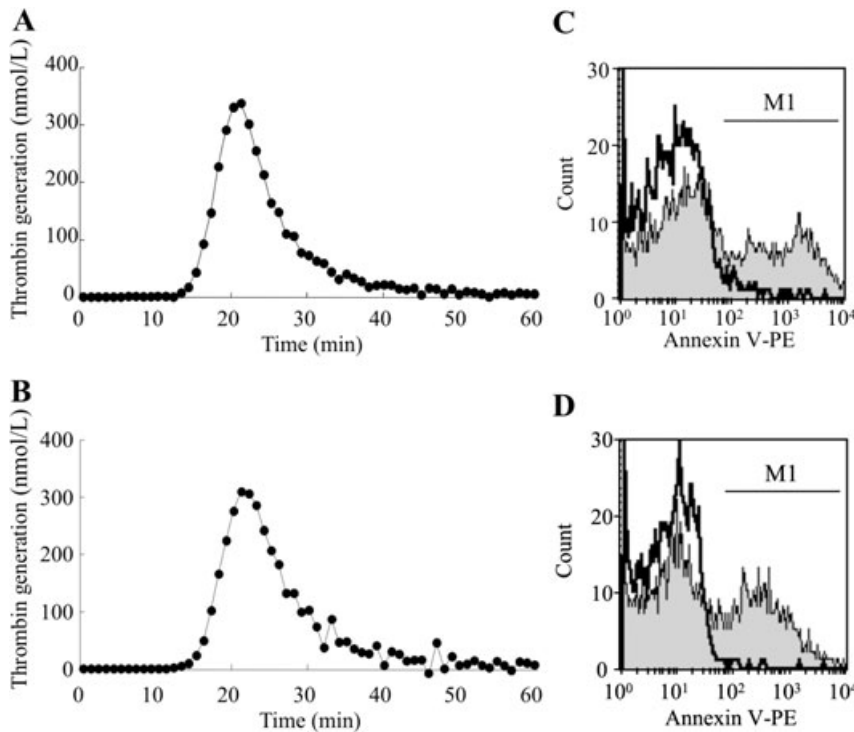


**Fig. 6.** In vitro thrombin generation and phosphatidylserine exposure of  $V_{sto}$  and  $V_{ca}$ . (A, B) After adjusting the number of vesicles to  $1 \times 10^4$ ,  $V_{ca}$  (A) and  $V_{sto}$  from RBC units stored for 50 days (B) were mixed with a thrombin-specific fluorogenic substrate and thrombin generation was started by adding human vesicle-free plasma to the mixture. The increase of the fluorescence signal was measured continuously, and the values were transformed into nmol per L thrombin equivalents with purified human  $\alpha$ -thrombin as a standard. (C, D) FACS analysis histograms are shown of  $V_{ca}$  (C) and  $V_{sto}$  from RBCs stored for 50 days (D) stained with annexin V-PE either in a calcium-containing buffer (closed histogram) or in a calcium-free buffer as control (open histogram). Representative data of a set of three experiments are shown.

our previous results on fresh RBCs,<sup>15</sup> we estimate stomatin to be 3-fold enriched in, and flotillin-2 to be 16-fold depleted from,  $V_{sto}$  compared to their respective protein-to-phospholipid ratios at the RBC membrane. Similar results were obtained by semiquantitative mass spectrometric analyses of stomatin and flotillin-2 comparing their relative amounts in the proteome of  $V_{sto}$  and RBC membranes (G.J. Bosman et al., manuscript in preparation).

What are the mechanisms by which these prominent RBC raft markers are segregated during the vesiculation process? In RBCs, there are limited possibilities that might account for the depletion of a membrane protein from a nascent vesicle. Cytoskeletal association of the respective membrane protein can inhibit the diffusion into the tip of the cytoskeleton-free membrane protrusion where the vesicles most likely originate. For example, the degree of band 3 depletion from  $V_{ca}$  correlates with its degree of association with the cytoskeleton.<sup>14</sup> Alternatively, steric constraints could inhibit a membrane-bound molecule or

molecular ensemble to enter the highly curved area at the tip of the echinocytic membrane protrusion.<sup>18</sup> Flotillins are monotopic membrane proteins present as oligomeric complexes at the cytoplasmic membrane leaflet and are assumed to be tightly associated with the cytoskeleton as suggested from studies on DRMs.<sup>20,49,50</sup> This cytoskeletal linkage is likely to contribute to the depletion of the flotillin proteins from  $V_{sto}$ .

But what is the driving force behind the enrichment of stomatin in the  $V_{sto}$  (Table 1, Fig. 4)? Stomatin is largely present in vesicular DRMs (Fig. 5) thereby indicating that the enrichment of stomatin in the vesicles is due to its raft association. There is growing evidence that lipid rafts are generally associated with membrane budding processes, including endocytosis and exocytosis, intracellular vesicle formation, and the release of virus particles from the plasma membrane.<sup>51-53</sup> Theoretical considerations<sup>54-56</sup> and recent studies on model membranes<sup>57</sup> indicate that membrane budding and eventual vesicle fission can occur upon large-scale separation of coexisting lipid phases. The generation of phase-separated domains in a multicomponent lipid bilayer membrane is driven by the minimization of the line tension at the phase boundary and is counter-

acted by the decrease in entropy due to the merger of smaller domains.<sup>58</sup> Because the entropic factor is temperature-dependent, the demixing of lipid phases is favored at low temperatures.<sup>59</sup> Extrapolating these considerations to RBC storage, one can assume that the stability of rafts and the tendency to form large raft aggregates is increased in the RBC membrane during storage of RBCs at 2 to 6°C. An updated model of lipid rafts<sup>52</sup> suggests that lipid rafts are small, mobile liquid-ordered domains that spontaneously form within the membrane and exist on short time scales. The stability of a short-lived raft, however, can be increased by interaction with a membrane protein and/or its attached lipid moieties. Protein-protein interaction can further increase stability and spatial extension of the raft domain. Stomatin fulfills both criteria as a raft-scaffolding protein,<sup>20,60,61</sup> being palmitoylated<sup>62</sup> and forming high-order homo-oligomers.<sup>63,64</sup> Thus stomatin-oligomers could be the nuclei for raft aggregations and local-phase demixing, which is further favored by the low storage temperatures. Budding and vesicle for-

mation, however, can only occur in membrane areas that are detached from the underlying cytoskeleton. RBC storage is associated with cytoskeletal changes such as abnormal spectrin-protein 4.1-actin complex formation, increased spectrin oxidation, and a loss in the band 3-ankyrin anchorage of the cytoskeleton to the lipid bilayer. All of these alterations are strongly correlated with vesiculation.<sup>3,4,8</sup> Recently, it was shown that the cytoskeleton is generally involved in the organization of membrane proteins in distinct raft and nonraft islands.<sup>65</sup> In view of the enrichment of stomatin in the  $V_{sto}$ , it is tempting to speculate that the storage-dependent cytoskeletal alterations impair the association of stomatin with the cytoskeleton. As outlined above, laterally mobile stomatin oligomers could then favor larger-scale phase separation and eventual vesicle formation.

The enrichment of stomatin in exovesicles might be also true for the pathologic condition of sickle cell disease, which is associated with excess surface area loss from RBCs due to vesiculation<sup>66</sup> and thereby might account for the significant depletion of stomatin from these cells.<sup>67</sup> Yet, storage and sickle cell pathology are likely to have different effects on membrane organization and vesicle formation. Because flotillin-1 is also reduced in sickle cells,<sup>67</sup> it is tempting to speculate that—in contrast to  $V_{ca}$  and  $V_{sto}$  from normal RBCs—sickle cell-derived vesicles might be also enriched in this protein. In general, we suggest that analyses of vesicular protein contents will provide important information on the respective vesiculation mechanism and the membrane architecture of the parent RBC in various (patho-)physiologic conditions.

## REFERENCES

1. Card RT. Red cell membrane changes during storage. *Transfus Med Rev* 1988;2:40-7.
2. Card RT, Mohandas N, Mollison PL. Relationship of post-transfusion viability to deformability of stored red cells. *Br J Haematol* 1983;53:237-40.
3. Wagner GM, Chiu DT, Qju JH, Heath RH, Lubin BH. Spectrin oxidation correlates with membrane vesiculation in stored RBCs. *Blood* 1987;69:1777-81.
4. Wolfe LC, Byrne AM, Lux SE. Molecular defect in the membrane skeleton of blood bank-stored red cells. Abnormal spectrin-protein 4.1-actin complex formation. *J Clin Invest* 1986;78:1681-6.
5. Knight JA, Voorhees RP, Martin L, Anstall H. Lipid peroxidation in stored red cells. *Transfusion* 1992;32:354-7.
6. Rumsby MG, Trotter J, Allan D, Michell RH. Recovery of membrane micro-vesicles from human erythrocytes stored for transfusion: a mechanism for the erythrocyte discocyte-to-spherocyte shape transformation. *Biochem Soc Trans* 1977;5:126-8.
7. Willekens FL, Werre JM, Kruijt JK, Roerdinkholder-Stoelwinder B, Groenen-Dopp YA, van den Bos AG, Bosman GJ, van Berkel TJ. Liver Kupffer cells rapidly remove red blood cell-derived vesicles from the circulation by scavenger receptors. *Blood* 2005;105:2141-5.
8. Bosman GJ, Willekens FL, Werre JM. Erythrocyte aging: a more than superficial resemblance to apoptosis? *Cell Physiol Biochem* 2005;16:1-8.
9. Iida K, Whitlow MB, Nussenzweig V. Membrane vesiculation protects erythrocytes from destruction by complement. *J Immunol* 1991;147:2638-42.
10. Greenwalt TJ, McGuinness CG, Dumaswala UJ. Studies in red blood cell preservation: 4. Plasma vesicle hemoglobin exceeds free hemoglobin. *Vox Sang* 1991;61:14-7.
11. Greenwalt TJ, Bryan DJ, Dumaswala UJ. Erythrocyte membrane vesiculation and changes in membrane composition during storage in citrate-phosphate-dextrose-adenine-1. *Vox Sang* 1984;47:261-70.
12. Oreskovic RT, Dumaswala UJ, Greenwalt TJ. Expression of blood group antigens on red cell microvesicles. *Transfusion* 1992;32:848-9.
13. Cole WF, Rumsby MG, Longster GH, Tovey LA. Changes in the inhibition of specific agglutination by plasma due to microvesicles released from human red cells during storage for transfusion. *Vox Sang* 1979;37:73-7.
14. Hagelberg C, Allan D. Restricted diffusion of integral membrane proteins and polyphosphoinositides leads to their depletion in microvesicles released from human erythrocytes. *Biochem J* 1990;271:831-4.
15. Salzer U, Prohaska R. Segregation of lipid raft proteins during calcium-induced vesiculation of erythrocytes [letter]. *Blood* 2003;101:3751-3.
16. Civenni G, Test ST, Brodbeck U, Butikofer P. In vitro incorporation of GPI-anchored proteins into human erythrocytes and their fate in the membrane. *Blood* 1998;91:1784-92.
17. Salzer U, Hinterdorfer P, Hunger U, Borker C, Prohaska R. Ca(++)-dependent vesicle release from erythrocytes involves stomatin-specific lipid rafts, synexin (annexin VII), and sorcin. *Blood* 2002;99:2569-77.
18. Hagerstrand H, Mrowczynska L, Salzer U, Prohaska R, Michelsen KA, Kralj-Iglic V, Iglic A. Curvature-dependent lateral distribution of raft markers in the human erythrocyte membrane. *Mol Membr Biol* 2006;23:277-88.
19. Salzer U, Ahorn H, Prohaska R. Identification of the phosphorylation site on human erythrocyte band 7 integral membrane protein: implications for a monotopic protein structure. *Biochim Biophys Acta* 1993;1151:149-52.
20. Salzer U, Prohaska R. Stomatin, flotillin-1, and flotillin-2 are major integral proteins of erythrocyte lipid rafts. *Blood* 2001;97:1141-3.
21. Luten M, Roerdinkholder-Stoelwinder B, Bost HJ, Bosman GJ. Survival of the fittest?—survival of stored red blood cells after transfusion. *Cell Mol Biol (Noisy-le-Grand)* 2004;50:197-203.
22. Gyongyossy-Issa MI, Weiss SL, Sowemimo-Coker SO, Garcez RB, Devine DV. Prestorage leukoreduction and low-

- temperature filtration reduce hemolysis of stored red cell concentrates. *Transfusion* 2005;45:90-6.
23. Rapaille A, Moore G, Siquet J, Flament J, Sondag-Thull D. Prestorage leukocyte reduction with in-line filtration of whole blood: evaluation of red cells and plasma storage. *Vox Sang* 1997;73:28-35.
  24. de Korte D, Haverkort WA, van Gennip AH, Roos D. Nucleotide profiles of normal human blood cells determined by high-performance liquid chromatography. *Anal Biochem* 1985;147:197-209.
  25. de Korte D, Haverkort WA, Roos D, van Gennip AH. Anion-exchange high performance liquid chromatography method for the quantitation of nucleotides in human blood cells. *Clin Chim Acta* 1985;148:185-96.
  26. Han W, Lindsay SM, Jing T. A magnetically driven oscillating probe microscope for operation in liquid. *Appl Phys Lett* 1996;69:1-3.
  27. Raab A, Han W, Badt D, Smith-Gill SJ, Lindsay SM, Schindler H, Hinterdorfer P. Antibody recognition imaging by force microscopy. *Nat Biotechnol* 1999;17:901-5.
  28. Hinterdorfer P, Baumgartner W, Gruber HJ, Schilcher K, Schindler H. Detection and localization of individual antibody-antigen recognition events by atomic force microscopy. *Proc Natl Acad Sci U S A* 1996;93:3477-81.
  29. Hinterdorfer P, Schilcher K, Baumgartner W, Gruber HJ, Schindler H. A mechanistic study of the dissociation of individual antibody-antigen pairs by atomic force microscopy. *Nanobiology* 1998;4:39-50.
  30. Luddington R, Baglin T. Clinical measurement of thrombin generation by calibrated automated thrombography requires contact factor inhibition. *J Thromb Haemost* 2004;2:1954-9.
  31. Varadi K, Negrier C, Berntorp E, Astermark J, Bordet JC, Morfini M, Linari S, Schwarz HP, Turecek PL. Monitoring the bioavailability of FEIBA with a thrombin generation assay. *J Thromb Haemost* 2003;1:2374-80.
  32. Kienberger F, Stroh C, Kada G, Moser R, Baumgartner W, Pastushenko V, Rankl C, Schmidt U, Muller H, Orlova E, LeGrimellec C, Drenckhahn D, Blaas D, Hinterdorfer P. Dynamic force microscopy imaging of native membranes. *Ultramicroscopy* 2003;97:229-37.
  33. Murphy SC, Samuel BU, Harrison T, Speicher KD, Speicher DW, Reid ME, Prohaska R, Low PS, Tanner MJ, Mohandas N, Haldar K. Erythrocyte detergent-resistant membrane proteins: their characterization and selective uptake during malarial infection. *Blood* 2004;103:1920-8. Epub 2003 Oct 30.
  34. Lauer S, VanWye J, Harrison T, McManus H, Samuel BU, Hiller NL, Mohandas N, Haldar K. Vacuolar uptake of host components, and a role for cholesterol and sphingomyelin in malarial infection. *EMBO J* 2000;19:3556-64.
  35. Greenwalt TJ. The how and why of exocytic vesicles. *Transfusion* 2006;46:143-52.
  36. Leroyer AS, Isobe H, Leseche G, Castier Y, Wassef M, Mallat Z, Binder BR, Tedgui A, Boulanger CM. Cellular origins and thrombogenic activity of microparticles isolated from human atherosclerotic plaques. *J Am Coll Cardiol* 2007;49:772-7.
  37. Chung SM, Bae ON, Lim KM, Noh JY, Lee MY, Jung YS, Chung JH. Lysophosphatidic acid induces thrombogenic activity through phosphatidylserine exposure and procoagulant microvesicle generation in human erythrocytes. *Arterioscler Thromb Vasc Biol* 2007;27:414-21.
  38. Cole WF, Rumsby MG, Longster GH, Tovey LA. The release of erythrocyte membrane antigens to the plasma as membrane microvesicles during the storage of human blood for transfusion [proceedings]. *Biochem Soc Trans* 1978;6:1375-8.
  39. Laczko J, Szabolcs M, Jona I. Vesicle release from erythrocytes during storage and failure of rejuvenation to restore cell morphology. *Haematologia (Budap)* 1985;18:233-48.
  40. Greenwalt TJ, Zehner Sostok C, Dumaswala UJ. Studies in red blood cell preservation. 1. Effect of the other formed elements. *Vox Sang* 1990;58:85-9.
  41. Hess JR, Hill HR, Oliver CK, Lippert LE, Rugg N, Joines AD, Gormas JF, Pratt PG, Silverstein EB, Greenwalt TJ. Twelve-week RBC storage. *Transfusion* 2003;43:867-72.
  42. Hess JR, Rugg N, Gormas JK, Knapp AD, Hill HR, Oliver CK, Lippert LE, Silverstein EB, Greenwalt TJ. RBC storage for 11 weeks. *Transfusion* 2001;41:1586-90.
  43. Gov NS, Safran SA. Red blood cell membrane fluctuations and shape controlled by ATP-induced cytoskeletal defects. *Biophys J* 2005;88:1859-74.
  44. Sens P, Gov N. Force balance and membrane shedding at the red-blood-cell surface. *Phys Rev Lett* 2007;98:018102.
  45. Basse F, Stout JG, Sims PJ, Wiedmer T. Isolation of an erythrocyte membrane protein that mediates Ca<sup>2+</sup>-dependent transbilayer movement of phospholipid. *J Biol Chem* 1996;271:17205-10.
  46. Verhoeven AJ, Hilarius PM, Dekkers DW, Lagerberg JW, de Korte D. Prolonged storage of red blood cells affects aminophospholipid translocase activity. *Vox Sang* 2006;91:244-51.
  47. Butikofer P, Kuypers FA, Xu CM, Chiu DT, Lubin B. Enrichment of two glycosyl-phosphatidylinositol-anchored proteins, acetylcholinesterase and decay accelerating factor, in vesicles released from human red blood cells. *Blood* 1989;74:1481-5.
  48. Allan D, Thomas P, Limbrick AR. The isolation and characterization of 60 nm vesicles ("nanovesicles") produced during ionophore A23187-induced budding of human erythrocytes. *Biochem J* 1980;188:881-7.
  49. Ciana A, Balduini C, Minetti G. Detergent-resistant membranes in human erythrocytes and their connection to the membrane-skeleton. *J Biosci* 2005;30:317-28.
  50. Salzer U, Hunger U, Prohaska R. Insights in the organization and dynamics of erythrocyte lipid rafts. *Adv Planar Lipid Bilayers Liposomes* 2007;5:49-81.
  51. Huttner WB, Zimmerberg J. Implications of lipid micro-

- domains for membrane curvature, budding and fission. *Curr Opin Cell Biol* 2001;13:478-84.
52. Hancock JF. Lipid rafts: contentious only from simplistic standpoints. *Nat Rev Mol Cell Biol* 2006;7:456-62.
  53. Laliberte JP, McGinnes LW, Peeples ME, Morrison TG. Integrity of membrane lipid rafts is necessary for the ordered assembly and release of infectious Newcastle disease virus particles. *J Virol* 2006;80:10652-62.
  54. Lipowsky R. Budding of membranes induced by intramembrane domains. *J Phys II* 1992;2:1825-40.
  55. Julicher F, Lipowsky R. Domain-induced budding of vesicles. *Phys Rev Lett* 1993;70:2964-7.
  56. Julicher F, Lipowsky R. Shape transformations of vesicles with intramembrane domains. *Phys Rev E Stat Nonlin Soft Matter Phys* 1996;53:2670-83.
  57. Baumgart T, Hess ST, Webb WW. Imaging coexisting fluid domains in biomembrane models coupling curvature and line tension. *Nature* 2003;425:821-4.
  58. Frolov VA, Chizmadzhev YA, Cohen FS, Zimmerberg J. "Entropic traps" in the kinetics of phase separation in multicomponent membranes stabilize nanodomains. *Biophys J* 2006;91:189-205.
  59. Heerklotz H, Szadkowska H, Anderson T, Seelig J. The sensitivity of lipid domains to small perturbations demonstrated by the effect of Triton. *J Mol Biol* 2003;329:793-9.
  60. Snyers L, Umlauf E, Prohaska R. Association of stomatin with lipid-protein complexes in the plasma membrane and the endocytic compartment. *Eur J Cell Biol* 1999;78:802-12.
  61. Salzer U, Mairhofer M, Prohaska R. Stomatin: a new paradigm of membrane organization emerges. *Dynamic Cell Biol* 2007;1:20-33.
  62. Snyers L, Umlauf E, Prohaska R. Cysteine 29 is the major palmitoylation site on stomatin. *FEBS Lett* 1999;449:101-4.
  63. Snyers L, Umlauf E, Prohaska R. Oligomeric nature of the integral membrane protein stomatin. *J Biol Chem* 1998;273:17221-6.
  64. Umlauf E, Mairhofer M, Prohaska R. Characterization of the stomatin domain involved in homo-oligomerization and lipid raft association. *J Biol Chem* 2006;281:23349-56.
  65. Lillemeier BF, Pfeiffer JR, Surviladze Z, Wilson BS, Davis MM. Plasma membrane-associated proteins are clustered into islands attached to the cytoskeleton. *Proc Natl Acad Sci U S A* 2006;103:18992-7.
  66. Wagner GM, Schwartz RS, Chiu DT, Lubin BH. Membrane phospholipid organization and vesiculation of erythrocytes in sickle cell anaemia. *Clin Haematol* 1985;14:183-200.
  67. Kakhniashvili DG, Griko NB, Bulla LA Jr, Goodman SR. The proteomics of sickle cell disease: profiling of erythrocyte membrane proteins by 2D-DIGE and tandem mass spectrometry. *Exp Biol Med (Maywood)* 2005;230:787-92. 